

The Origin of Cosmic Dust.

Loretta Dunne*, Stephen Eales*, Rob Ivison[†], Haley Morgan*, Mike Edmunds*

**Department of Physics & Astronomy, Cardiff University, 5 The Parade, Cardiff CF24 3YB,*

UK

[†]Astronomy Technology Centre, Royal Observatory, Blackford Hill, Edinburgh EH9 3HJ, UK

Large amounts of dust ($> 10^8 M_\odot$) have recently been discovered in high redshifts quasars^{1,2} and galaxies^{3–5}, corresponding to a time when the Universe was less than one-tenth of its present age. The stellar winds produced by stars in the late stages of their evolution (on the asymptotic giant branch of the Hertzsprung-Russell diagram) are thought to be the main source of dust in galaxies, but they cannot produce that dust on a short-enough timescale⁶ (< 1 Gyr) to explain the results in the high-redshift galaxies. Supernova explosions of massive stars (type II) are also a potential source, with models predicting $0.2\text{--}4 M_\odot$ of dust^{7–10}. As massive stars evolve rapidly, on timescales of a few Myr, these supernovae could be responsible for the high-redshift dust. Observations^{11–13} of supernova remnants in the Milky Way, however, have hitherto revealed only $10^{-7} - 10^{-3} M_\odot$ of dust each, which is insufficient to explain the high-redshift data. Here we report the detection of $\sim 2\text{--}4 M_\odot$ of cold dust in the youngest known Galactic remnant, Cassiopeia A. This observation implies that supernovae are at least as important as stellar winds in producing dust in our Galaxy and would have been the dominant source of dust at high redshifts.

Over the past three decades, many searches for dust in supernova remnants (SNR) have been made in the mid and far-infrared ($6\text{--}100\mu\text{m}$). Remnants must be studied when they are young, before they have swept up large masses of interstellar material which makes it difficult to distinguish dust formed in the ejecta from that present in the ISM prior to the explosion. The handful of Galactic remnants which are both young and close enough (Cas A, Kepler and Tycho) have been studied with the Infrared Astronomical Satellite (IRAS) and the Infrared Space Observatory (ISO), but although dust at $100\text{--}200$ K has been detected, the dust mass deduced is only $10^{-7} - 10^{-3} M_\odot$, many orders of magnitude lower than the solar mass quantities predicted.^{11–13} The formation of dust in the recent supernova 1987A has been implied indirectly from the fading of the silicate line and increase in $10\mu\text{m}$ emission,¹⁴ although the quantity is heavily dependant on the assumptions made

about the clumpiness of the dust*. The IRAS/ISO observations were not sensitive to cold dust at ≤ 25 K, if the models are correct about the amount of dust produced in supernovae (SNe) then the bulk of the dust must be cold. Such dust will emit most of its radiation at longer wavelengths and so the best place to search for cold dust emission is at sub-millimetre (submm) wavelengths (0.3–1 mm). Here, we present our analysis of submm data for Cassiopeia A, the youngest known Galactic remnant. Cas A is the brightest radio source in the sky, and still produces significant synchrotron emission at submm wavelengths. Cas A is believed to be the remnant of the explosion of a massive (20–30 M_{\odot}) progenitor star, which occurred around 320–340 yrs ago at a distance of 3.4 kpc.^{15,16}

Cas A was observed with the SCUBA¹⁷ array on the JCMT in June 1998. The 850 μ m image is presented in Fig. 1 and shows a ring-like morphology, similar to the X-ray and radio images^{18,19}. Over two-thirds of the 850 μ m emission in the main ring is synchrotron produced by relativistic electrons spiralling in the intense magnetic field. Fig. 2 presents the spectral energy distribution (SED) of Cas A from the radio to the mid-IR, showing the clear excess due to dust at wavelengths of $\leq 850\mu$ m. The synchrotron radiation displays a constant power-law behaviour over more than two decades in frequency with $S_{\nu} \propto \nu^{\alpha}$ where $\alpha = -0.72$, meaning that its contribution to the submm flux can be easily estimated and subtracted. The 450 μ m image is shown in Fig. 3, the synchrotron contribution is now only one third and emission from cold dust dominates which is why the 450 and 850 μ m images appear different. We can remove the synchrotron contribution from the submm maps by scaling an 83 GHz image,¹⁹ which is the closest in frequency and resolution to our images. Fig. 4 shows the result with contours denoting the 450 μ m synchrotron subtracted flux. The general similarity between the two wavelengths, once the synchrotron has been removed, is strong evidence that this is indeed emission from cold dust.

The rings on Fig. 4 indicate the position of the forward and reverse shocks as determined from Chandra X-ray data.¹⁸ Most of the dust appears to be contained between the two, where the gas density as traced by the X-rays is greatest. We fitted a two-temperature grey body SED to the synchrotron corrected IR/submm fluxes (Fig. 2) determining temperatures of 112 K and 18 K for the two components. The SED parameters and their uncertainties are given in Table 1. The temperature of the hot dust is easily explained if it is co-extensive with the X-ray emitting gas ($10^6 - 10^7$ K) and is heated by collisions with fast moving electrons and ions¹³. The cold dust could be explained in a number of ways and a more detailed investigation will be presented elsewhere (Dunne et al. in prep). If the grains are very small ($< 0.005\mu$ m) they may cool to 15–20 K in the time between collisions with the gas particles. However, the dust SED might then be expected to show dust at all

*If the dust is uniform, the observations imply a very low efficiency of condensation of heavy elements into dust grains ($\sim 0.001\%$), while if dust is very clumped this could rise to almost 100% in some species

temperatures between 100-20 K, which is not apparent. Alternatively, the cold dust may be located in a very hot but diffuse phase of the gas, surrounding the bright, dense X-ray filaments. If the gas had a density of $< 0.01 \text{ cm}^{-3}$ then the grains could be this cold. The dust could also be contained in dense clumps which are not in pressure equilibrium with the more diffuse X-ray gas, a model which has been suggested for SN 1987A¹⁴. Finally, the cold dust could be in thermal equilibrium with the same X-ray gas which is responsible for heating the hot dust, if the cold grains are both very large ($1\text{-}10\mu\text{m}$) and emit more efficiently than grains in the diffuse ISM. Evidence for unusual grain properties in Cas A is presented below.

The mass of dust can be estimated from the submm emission using $M_d = \frac{S_\nu D^2}{\kappa_\nu B(\nu, T)}$, where D is the distance to the remnant (3.4 kpc), $B(\nu, T)$ is the Planck function at temperature T and κ is the dust mass absorption coefficient. The submm emission is clearly dominated by the cold dust, therefore the cold temperature is the only one we need be concerned with. The value of κ is the main uncertainty as its value is not well determined and may vary with physical environment. Dust masses derived from the SED and different values of κ are in Table 1. Using ‘standard’ κ values appropriate to the diffuse ISM²⁰ (κ_3) gives dust masses which are uncomfortably high ($> 7 M_\odot$). Higher κ values, as measured in environments where dust may be newly formed, amorphous or coagulated (see Table 1) produce more sensible estimates ($2 - 6 M_\odot$), thus the dust in Cas A appears to have different properties to that in the diffuse ISM. It is possible that grain processing in the diffuse ISM by UV photons and passage through dark clouds may alter the surface chemistry or shape of grains, causing a change in their emissivity. At an age of 320 yrs, the dust in Cas A is relatively pristine and has not yet been subjected to the above events, this may contribute to its greater emissivity.

Was the dust produced in the supernova explosion, or could it be pre-existing dust which was swept up by the blast wave? If the remnant has swept up ISM material with a uniform density¹⁹ of $0.4\text{--}4 \text{ H atoms per cm}^{-3}$ then only $0.004 - 0.04 M_\odot$ of dust should be present[†]. Higher ISM densities are possible, but in order for the mass of dust inferred in Cas A to have been swept up densities of the order $200\text{--}400 \text{ cm}^{-3}$ are required. This would mean Cas A has swept up $\sim 200 - 400 M_\odot$ of material which is inconsistent with its dynamical state^{18,21}, believed to be just entering the Sedov stage (i.e. it has swept up about as much mass as it ejected ($< 15 M_\odot$)). Another hypothesis for the bright ring seen in the X-ray and radio is that it is the interaction of the supernova with a stellar wind shell swept up by the Wolf-Rayet precursor^{16,22}. In this case, one could estimate that somewhere between $4\text{--}16 M_\odot$ of material could have been lost in the red-supergiant phase and swept up into the ring. For this to be the source of the dust we observe requires an implausibly large quantity of *freshly synthesised* elements efficiently condensing into dust in the stellar wind material⁶ (which, unlike the

[†]for an ISM gas-to-dust ratio of 160

supernova ejecta, is mainly H and He). We conclude that the most likely explanation for the large mass of dust in Cas A is that it was formed as a result of the supernova explosion.

Using our result, we estimate the current Galactic dust production rate from Type-II SNe as $7 - 18 (\times 10^{-3}) M_{\odot} \text{ yr}^{-1}$. Stellar wind⁶ sources produce $\sim 5 \times 10^{-3} M_{\odot} \text{ yr}^{-1}$, meaning that SNe are the dominant source of interstellar dust during most of galactic evolution. We have shown here that individual SNe are capable of producing of order of a solar mass of dust in the short times available in the early universe and therefore the dust observed at high redshift is likely to have originated in supernovae.

References

1. Bertoldi, F. *et al.* Dust emission from the most distant quasars. *Astron. Astrophys. Lett.* in the press; also available as preprint astro-ph/0305116 at <http://www.arXiv.org> (2003).
2. Archibald, E. N. *et al.* A submillimetre survey of the star formation history of radio galaxies. *Mon. Not. R. Astron. Soc.* **323**, 417-444 (2001).
3. Hughes, D. H. *et al.* High-redshift star formation in the Hubble Deep Field revealed by a submillimetre-wavelength survey. *Nature.* **394**, 241-247 (1998).
4. Smail, I., Ivison, R. J. & Blain, A. W. A Deep Sub-millimeter Survey of Lensing Clusters: A New Window on Galaxy Formation and Evolution. *Astrophys. J.* **490**, L5-L8 (1997).
5. Dunne, L., Eales, S. A. & Edmunds, M. G. A census of metals at high and low redshifts and the connection between submillimetre sources and spheroid formation. *Mon. Not. R. Astron. Soc.* **341** 589-598 (2003).
6. Morgan, H. L. & Edmunds M. G. Dust Formation in Early Galaxies. *Mon. Not. R. Astron. Soc.* in the press; also available as preprint astro-ph/0302566 at <http://www.arXiv.org> (2003).
7. Todini, P. & Ferrara, A. Dust Formation in primordial Type II supernovae. *Mon. Not. R. Astron. Soc.* **325**, 726-736 (2001).
8. Clayton, D. D., Liu, W. & Dalgarno, A. Condensation of Carbon in Radioactive Supernova Gas. *Science* **283**, 1290-1292 (1999).
9. Kozasa, T., Hasegawa, H. & Nomoto, K. Formation of dust grains in the ejecta of SN 1987A. II *Astron. Astrophys.* **249**, 474-482 (1991).

10. Woosley, S. E. & Weaver, T. A. The Evolution and Explosion of Massive Stars. II. Explosive Hydrodynamics and Nucleosynthesis. *Astrophys. J. Sup. Ser.* **101**, 101-181 (1995).
11. Lagage, P. O. *et al.* Dust Formation in the Cassiopeia A supernova. *Astron. Astrophys.* **315**, L273-L276 (1996).
12. Douvion, T, Lagage, P. O., Cesaesky, C. J., Dwek, E. Dust in the Tycho, Kepler and Crab supernova remnants. *Astron. Astrophys.* **373**, 281-291 (2001).
13. Dwek, E., Dinerstein, H. L., Gillet, F. C., Hauser, M. G., Rice, W. L. Physical processes and infrared emission from the Cassiopeia A supernova remnant. *Astrophys. J.* **315**, 571-579 (1987).
14. Lucy, L. B., Danziger, I. J., Gouiffes, C., Bouchet, P. Dust Condensation in the ejecta of SN 1987A, II. in *Supernovae. The Tenth Santa Cruz Workshop in Astronomy and Astrophysics* (ed. Woosley, S. E.) p.82 (New York, Springer-Verlag, 1991).
15. Reed, J. E., Hester, J. J., Fabian, A. C., Winkler, P. F. The three-dimensional structure of the Cassiopeia A supernova remnant. I. The spherical shell. *Astrophys. J.* **440**, 706-721 (1995).
16. García-Segura, G., Langer, N. & MacLow, M.-M. The hydrodynamic evolution of circumstellar gas around massive stars. *Astron. Astrophys.* **316**, 133-146 (1996).
17. Holland, W. S. *et al.* SCUBA: a common-user submillimetre camera operating on the James Clerk Maxwell Telescope. *Mon. Not. R. Astron. Soc.* **303**, 659-672 (1999).
18. Gotthelf, E. V. *et al.* CHANDRA detection of the forward and reverse shocks in Cassiopeia A. *Astrophys. J.* **552**, L39-L43 (2001).
19. Wright, M., Dickel, J., Koralesky, B., Rudnick, L. The supernova remnant Cassiopeia A at millimetre wavelengths. *Astrophys. J.* **518**, 284-297 (1999).

20. Li, A. & Draine, B. T. Infrared Emission from Interstellar Dust. II. The Diffuse Interstellar Medium. *Astrophys. J.* **554** 778-802 (2001).
21. Agüeros, M. A., Green, D. A. The bulk expansion of the supernova remnant Cassiopeia A at 151 MHz. *Mon. Not. R. Astron. Soc.* **305** 957-965 (1999).
22. Borkowski, K. J., Szymkowiak, A. E., Blondin, J. M., Sarazin, C. L. A circumstellar shell model for the Cassiopeia A supernova remnant. *Astrophys. J.* **466** 866-870 (1996).
23. Reichart, D. E. & Stephens, A. W. The Fading of Supernova Remnant Cassiopeia A from 38 MHz to 16.5 GHz from 1949 to 1999 with New Observations at 1405 MHz. *Astrophys. J.* **537**, 904-908 (2000).
24. Baars, J. W. M., Genzel, R., Pauliny-Toth, I. I. K., Witzel, A. The absolute spectrum of CAS A - an accurate flux density scale and a set of secondary calibrators. *Astron. & Astrophys.* **61**, 99-106 (1977).
25. O'Sullivan, C. & Green, D. A. Constraints on the secular decrease in the flux density of CAS A at 13.5, 15.5 and 16.5 GHz. *Mon. Not. R. Astron. Soc.* **303**, 575-578 (1999).
26. Mason, B. S. *et al.* An Absolute Flux Density Measurement of the Supernova Remnant Cassiopeia A at 32 GHz. *Astron. J.* **118**, 2908-2918 (1999).
27. Liszt, H. & Lucas, R. 86 and 140 GHz radiocontinuum maps of the Cassiopeia A SNR. *Astron. Astrophys.* **347**, 258-265 (1999).
28. Mezger, P. G., Tuffs, R. J., Chini, R., Kreysa, E., Gemuend, H.-P. Maps of Cassiopeia A and the Crab Nebula at lambda 1.2 MM. *Astron. Astrophys.* **167**, 145-150 (1986).
29. Saken, J. M., Fesen, R. A. & Shull, J. M. An IRAS survey of Galactic supernova remnants.

Astrophys. J. Supp. Ser. **81**, 715-745 (1992).

30. Tuffs, R. J. *et al.* The heating and origin of grains in Cassiopeia A and SN 1987A. in *The Universe as Seen by ISO* (eds. Cox, P. & Kessler, M. F.) p. 241-254 (ESA-SP 427, ESA Publications Division, ESTEC, Noordwijk, 1999).

Aknowledgments

We wish to thank Melvyn Wright for kindly providing us with the 83 GHz image, and Walter Gear and Dave Green for useful discussions. LD is supported by a PPARC postdoctoral fellowship and HM by a Cardiff University studentship. We are grateful to Gary Davis for use of Director's time on the JCMT to obtain the new photometry data.

The authors declare that they have no competing financial interests.

Correspondence and requests for materials should be addressed to Loretta Dunne (L.Dunne@astro.cf.ac.uk).

Table 1: **Properties of Cas A**

SED parameters			Dust masses (M_{\odot})		
β	T_{hot} (K)	T_{cold} (K)	κ_1	κ_2	κ_3
$0.9^{+0.8}_{-0.6}$	112^{+11}_{-21}	$18.0^{+2.6}_{-4.6}$	$M_{450} = 2.2^{+1.2}_{-0.2}$	$M_{450} = 3.8^{+2.0}_{-0.4}$	$M_{450} = 12.7^{+6.9}_{-1.1}$
			$M_{850} = 2.4^{+0.7}_{-0.3}$	$M_{850} = 6.2^{+1.7}_{-0.9}$	$M_{850} = 26.0^{+6.4}_{-4.1}$

SED parameters are the best least-squares fit to the data points. The errors were estimated using a bootstrap procedure in which the measured fluxes were perturbed according to their Gaussian errors and re-fitted to find new parameters. The process was repeated 3000 times and the uncertainties quoted are the 68% confidence interval derived from this method. Quoted dust masses are those from the best-fit SED parameters for each value of κ , and the ranges reflect the 68% confidence interval using the distribution produced by the bootstrap, essentially the uncertainty in dust mass due to the uncertainty in fluxes and SED fitting. We have used three values of κ which represent the average from numerous source in the literature for different grain environments (to be presented in more detail elsewhere, Dunne et al. in prep). (1) Laboratory measurements and theoretical modelling suggest that if grains are amorphous or have a clumpy, aggregate structure κ can be very high $0.6 - 1.1 \text{ m}^2 \text{ kg}^{-1}$ at $850 \mu\text{m}$. We take $\kappa_1(450) = 1.5 \text{ m}^2 \text{ kg}^{-1}$, $\kappa_1(850) = 0.76 \text{ m}^2 \text{ kg}^{-1}$. (2) Environments where dust may be newly formed, or modified by icy mantles also show high values $0.16 - 0.8 \text{ m}^2 \text{ kg}^{-1}$. From observations of evolved stars, VRN (visual reflection nebulae), planetary nebulae and cold clouds in the Galaxy we take $\kappa_2(450) = 0.88 \text{ m}^2 \text{ kg}^{-1}$, $\kappa_2(850) = 0.3 \text{ m}^2 \text{ kg}^{-1}$. (3) Studies of extragalactic systems and diffuse ISM dust in the Galaxy support lower values of κ in the region of $0.04 - 0.15 \text{ m}^2 \text{ kg}^{-1}$ at $850 \mu\text{m}$. We take $\kappa_3(450) = 0.26 \text{ m}^2 \text{ kg}^{-1}$, $\kappa_3(850) = 0.073 \text{ m}^2 \text{ kg}^{-1}$.

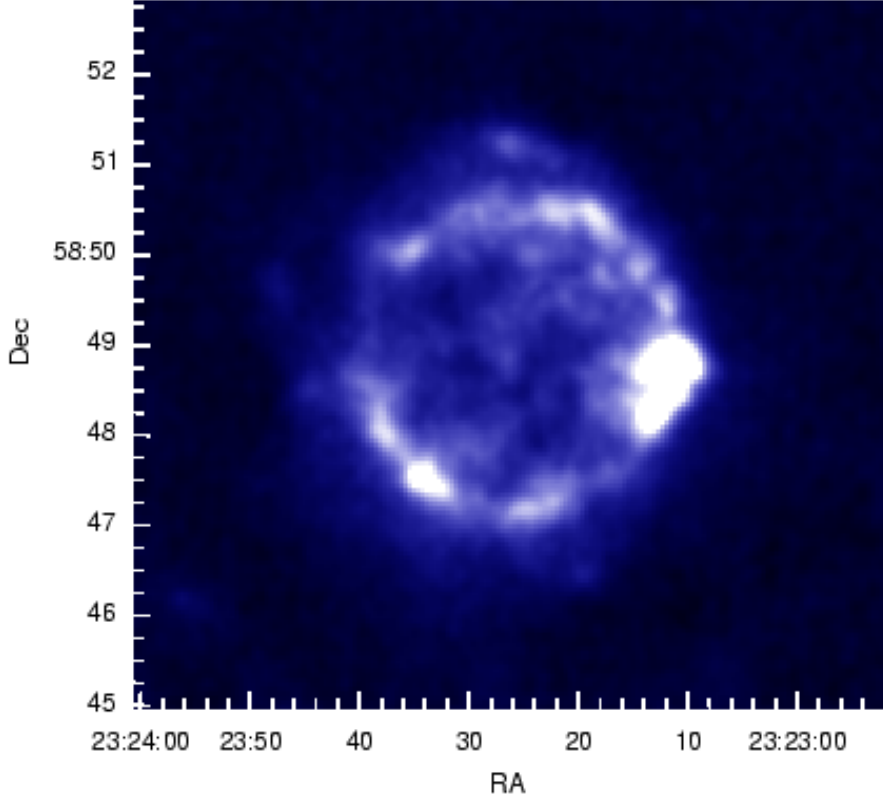


Figure 1: SCUBA $850\mu\text{m}$ image of Cas A at a resolution of 15 arcsec. The data were taken in scan map mode and reduced in a standard way using SURF. Scan map is known to produce artifacts on large angular scales on the final image and these remain the limitation on the accuracy of the absolute flux measurement and morphology. On the $850\mu\text{m}$ image, the linear baseline removal left an area of diffuse emission to the west of the remnant which we believe was an artifact. After subtraction of a surface which removed this feature the loss of flux in the remnant was 5 Jy. We confirmed the accuracy of the absolute flux level of the maps by making new photometric measurements with SCUBA at several positions on the remnant in December 2002. The quoted 1σ uncertainty on the fluxes is a combination of calibration errors (5–10% and 15–20% at $850/450\mu\text{m}$), plus the range of fluxes from the maps which agreed with the photometry. The integrated fluxes in were corrected for the error lobe contribution (derived from maps of Uranus) by dividing by 1.2 at $850\mu\text{m}$ and 2.0 at $450\mu\text{m}$.

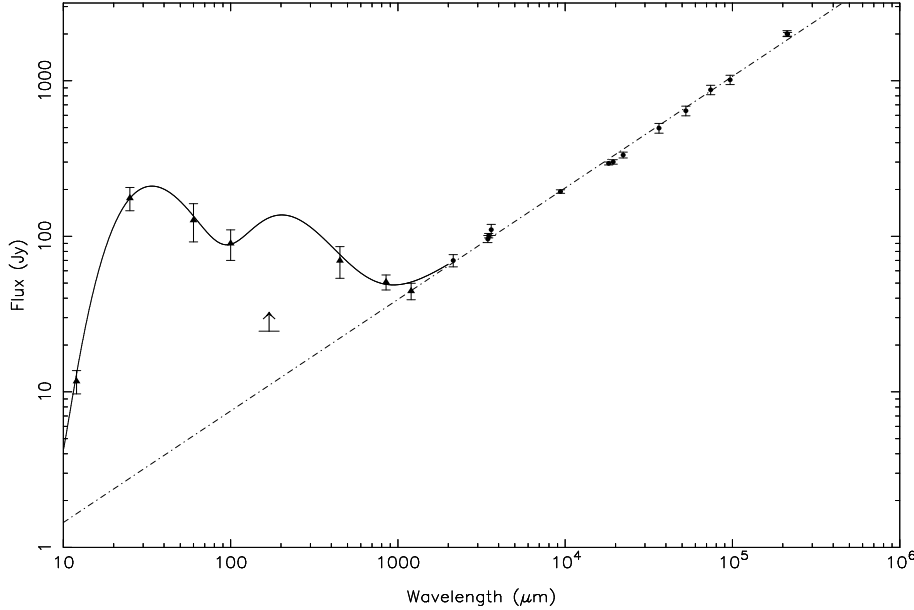


Figure 2: The SED of Cas A from the mid-IR to the radio. All fluxes are integrated. The radio spectrum is fitted with a power law slope with spectral index $\alpha = -0.72$. The radio data^{19,23–28} have been scaled to the epoch of our Cas A observation (1998.4) using a recent study²⁴ which found that the flux decrease of Cas A was independent of frequency at $\approx 0.6 - 0.7\%\text{yr}^{-1}$. The IRAS points are the averages of the literature values^{13,29} with the error bars indicating the range of fluxes. SCUBA fluxes are 50.8 ± 5.6 Jy at $850\mu\text{m}$ and 69.8 ± 16.1 Jy at $450\mu\text{m}$. The synchrotron contribution is 34.9 Jy at $850\mu\text{m}$ and 22.1 Jy at $450\mu\text{m}$. The fit to the FIR/submm points is for a 2 temperature grey-body with $\beta = 0.9$, $T_w = 112$ K, $T_c = 18$ K and for 700 times more mass in the cold component than in the hot. We have fitted 5 parameters to 6 data points and therefore the fit is just constrained. The uncertainties in the SED parameters are given in Table 1. Clearly, the submm points at 450 and $850\mu\text{m}$ lie above the extrapolation of the radio synchrotron spectrum. The point at 1.2mm (ref. 28) is not of sufficient accuracy to determine an excess, but is consistent with our higher frequency measurements. Longer wavelength ISO measurements³⁰ of Cas A at $170\mu\text{m}$ suggested that dust at ~ 30 K may have been present (implying of order $0.15 M_\odot$ of dust), however the poor angular resolution of ISO at these wavelengths made a separation of the remnant and background emission impossible. The ISO flux is therefore a lower limit (R. J. Tuffs, private communication).

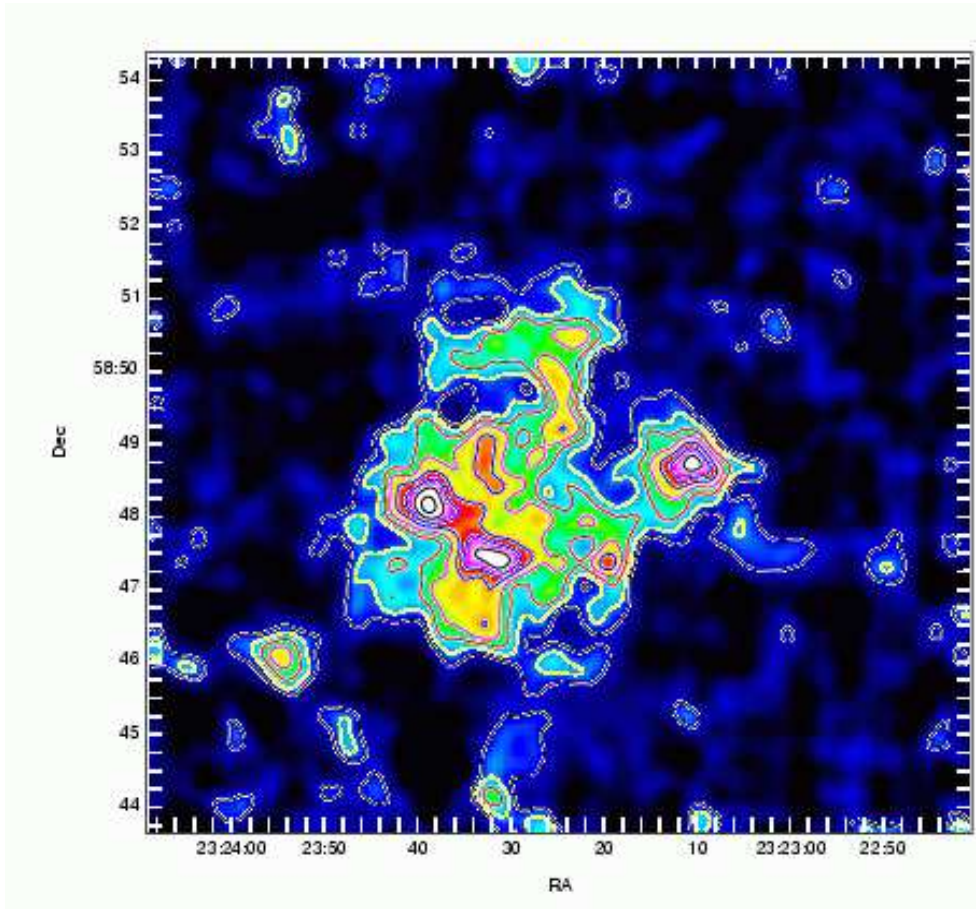


Figure 3: SCUBA $450\mu\text{m}$ map, smoothed with a $21''$ gaussian. Colours and contours both represent the $450\mu\text{m}$ emission. Contours start at 2σ , with intervals of 1σ . The difference in morphology between this image and that at $850\mu\text{m}$ (Fig. 1) is because emission from cold dust dominates at $450\mu\text{m}$, while two-thirds of the emission at $850\mu\text{m}$ is synchrotron.

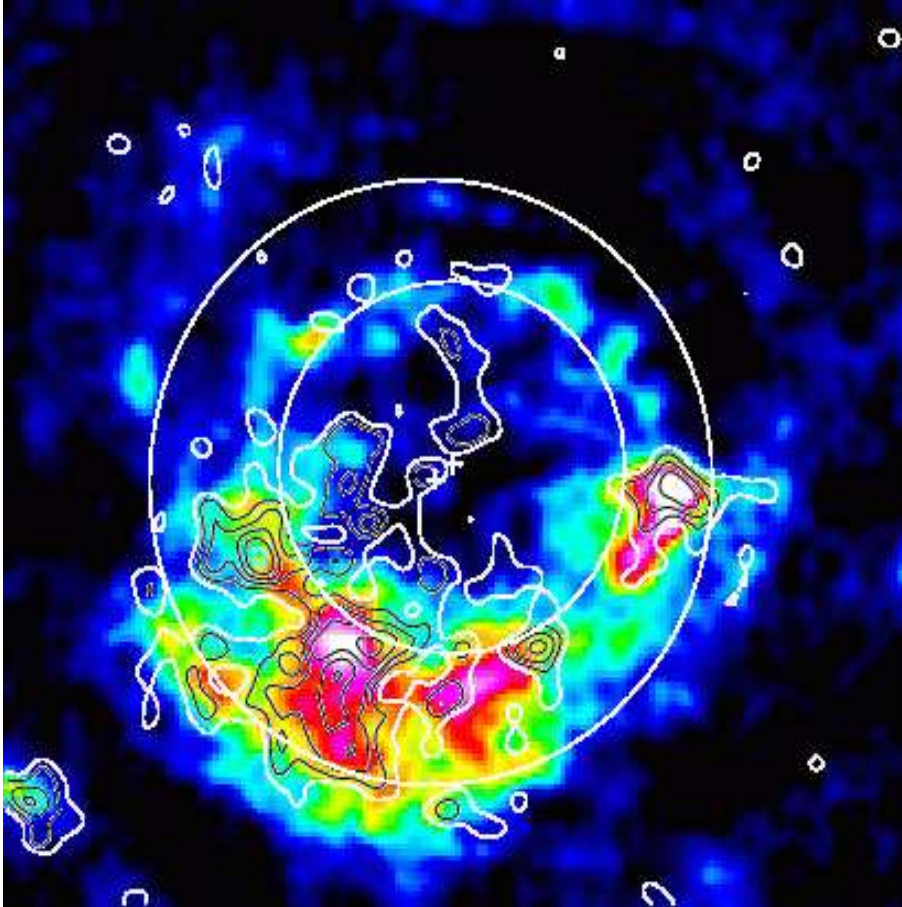


Figure 4: The $850\mu\text{m}$ emission once the synchrotron has been subtracted using an 83 GHz image¹⁹. The box is 8.4 arcmin by 7.8 arcmin, north is up and east is left. Colours represent the $850\mu\text{m}$ intensity, contours are the $450\mu\text{m}$ emission with the synchrotron subtracted, starting at 3σ with increments of $+1\sigma$. The rings and crosses indicate the location (and centroids) of the forward and reverse shocks as determined from Chandra X-ray data¹⁸. The forward shock is at a mean radius of $153\pm12''$ and the reverse shock is at a mean radius of $95\pm10''$. The bulk of the dust emission appears to be bounded by the shocks, where the gas density is highest. There is a noticeable asymmetry in the dust emission.